CANONICAL NONLINEAR PROGRAMMING CIRCUITS

by

J. L. Huertas, A. Rueda, A. Rodriguez-Vazquez

and L. O. Chua

Memorandum No. M85/100

19 December 1985

CANONICAL NONLINEAR PROGRAMMING CIRCUITS

by

J. L. Huertas, A. Rueda, A. Rodriguez-Vazquez

and L. O. Chua

Memorandum No. M85/100

19 December 1985

ELECTRONICS RESEARCH LABORATORY

College of Engineering
University of California, Berkeley
94720

CANONICAL NONLINEAR PROGRAMMING CIRCUITS †

by

J.L. Huertas, A. Rueda , A. Rodriguez-Vazquez (*)

and

L.O. Chua (**)

(*)Departamento de Electricidad y Electronica. Facultad de Fisica.

University of Seville, Seville, Spain

(**)Department of Electrical Engineering and Computer Science.

University of California, Berkeley, CA 94720.

†This work was supported in part by Office of Naval Research Contract N00014-70-C-0572 and National Science Foundation Grant ECS-8313278.

ABSTRACT

Several new canonical circuits for solving nonlinear programming problems in real time are presented. The solution of these circuits coincides with the stationary point of circuit's potential function, which is shown to exist even though it contains non-reciprocal circuit elements. Each canonical circuit is shown to impose the Kuhn-Tucker conditions for solving nonlinear programming problems.

CANONICAL NONLINEAR PROGRAMMING CIRCUITS

1. INTRODUCTION

Obtaining real-time solutions to nonlinear programming problems is required in some engineering systems (robotic, satellite guidance, etc.). Recently, a special circuit has been proposed [1] that allows us to solve such problems by analog simulation. This circuit is made of ideal diodes, nonlinear VCCS's and nonlinear CCVS's, and is capable of simulating any nonlinear programming problem in a systematic way. The fundamental property of the circuit in [1] is its relationship to the Kuhn-Tucker conditions for solving nonlinear programming problems. This relationship was shown to result from the fact that the circuit posseses a stationary property [2], although it contains some nonreciprocal circuit elements.

Our purpose in this paper is to show that there exist other circuits that exhibit the same remarkable properties and hence can also be used to solve any nonlinear programming problems. The new circuits are canonic in the same sense as defined in [1], but, as we shall see later on, two of them require only one type of controlled sources, thus making these circuits more attractive from an implementation point of view.

2. CANONIC NONLINEAR PROGRAMMING CIRCUITS: STATIONARY PROPERTY

Consider the general nonlinear programming problem of minimizing a scalar function $\phi(x_1, x_2, \ldots x_q)$, subject to the constraints $f_j(x_1, x_2, \ldots x_q) \geq 0$ $(1 \leq j \leq p)$, where q and p are independent integers.

The circuit in Fig. 1(a), whith x_k denoting the voltage v_k measured at the k-th node on the right-hand side subcircuits, is known to solve the above optimization problem [1]: The solution of this circuit is a stationary point of its total cocontent function, and hence, provided that $\phi(.)$ has only one stationary point and is a local minimum, that point is the global minimum of $\phi(.)$.

In this section, we will show that the new circuits proposed in Figures 1(b) to 1(d) also exhibit similar properties and can be used for solving the same nonlinear programming problems. In order to present the proof in a unified way, valid for all four circuits in Fig. 1, let us redraw them as an interconnection of two q-ports, N_a and N_b; and use the generic symbol x_k to denote the "controlling" port variable and the variable y_k to denote the "controlled" port variable for each n-port.

N_a is a q-port made of q nonlinear controlled sources on the right-hand side of each sub-circuit in Fig. 1. For the circuits in Fig. 1(a) and 1(c), they are controlled current sources, and for the circuits in Fig. 1(b) and 1(d), they are controlled voltage sources. Each of these four x-controlled q-ports N_a is characterized by

$$y_{ak} = \frac{\partial \phi(x_{a1}, x_{a2}, \ldots x_{aq})}{\partial x_{ak}} \quad , \quad k = 1,2,\ldots q \qquad (1)$$

N_b is a q-port made of the remaining circuit. In order to describe N_b as an x-controlled q-port, let us first "model" each ideal diode by a voltage-controlled resistor in Fig. 1(a) and 1(b), and by a current-controlled resistor in Fig. 1(c) and 1(d), respectively. In particular, model each ideal diode in Fig. 1(a) and 1(b) by

$$i_{d\ell} = g(v_{d\ell}) = \begin{cases} 0 & , \quad v_{d\ell} < 0 \\ \dfrac{1}{R_F}\, v_{d\ell} & , \quad \text{otherwise} \end{cases} \tag{2}$$

and that in Fig. 1(c) and 1(d) by

$$v_{d\ell} = g(i_{d\ell}) = \begin{cases} 0 & , \quad i_{d\ell} < 0 \\ \dfrac{1}{G_B}\, i_{d\ell} & , \quad \text{otherwise} \end{cases} \tag{3}$$

Using the above notation and model, each of the four x-controlled q-ports N_b is characterized by

$$y_{bk} = \sum_{\ell=1}^{p} -g[-f_\ell(x_{b1}, x_{b2}, \ldots x_{bq})] \frac{\partial f_\ell(x_{b1}, x_{b2}, \ldots x_{bq})}{\partial x_{bk}} \tag{4}$$

$$1 \leq k \leq q$$

where y_{bk} now denotes the current entering port k of N_b.

Assuming that the functions $\phi(.)$ and $f_\ell(.)$ are twice continously differentiable, we will now prove that both n-ports N_a and N_b are reciprocal. Indeed, for N_a we have from Eq.(1)

$$\frac{\partial y_{am}}{\partial x_{an}} = \frac{\partial \phi(x_{a1}, x_{a2}, \ldots x_{aq})}{\partial x_{am}\, \partial x_{an}} = \frac{\partial y_{an}}{\partial x_{am}} \tag{5}$$

and for N_b, we obtain from Equations (2)-(4)

$$\frac{\partial y_{bn}}{\partial x_{bn}} = -\sum_{\ell=1}^{p} \left[\frac{\partial f_\ell}{\partial x_{bm}} \left(\frac{\partial g}{\partial f_\ell} \frac{\partial f_\ell}{\partial x_{bn}} \right) + g(-f_\ell) \frac{\partial^2 f_\ell}{\partial x_{bm} \partial x_{bn}} \right] \tag{6a}$$

$$\frac{\partial y_{bn}}{\partial x_{bm}} = -\sum_{\ell=1}^{p} \left[\frac{\partial f_\ell}{\partial x_{bn}} \left(\frac{\partial g}{\partial f_\ell} \frac{\partial f_\ell}{\partial x_{bm}} \right) + g(-f_\ell) \frac{\partial^2 f_\ell}{\partial x_{bn} \partial x_{bm}} \right] \tag{6b}$$

It follows from the above that the Jacobian matrices of both N_a

and N_b are symmetric, and therefore both q-ports are reciprocal.

Since N_a and N_b are both reciprocal and homogeneously controlled (either current-controlled or voltage-controlled), we can define a potential function associated with each q-port, namely, $P_a(\underset{\sim}{x}_a)$ and $P_b(\underset{\sim}{x}_b)$. For the cases where $\underset{\sim}{x}$ is a voltage vector (Fig. 1(a) and 1(c)), these potential functions are the cocontents of N_a and N_b, respectively [2]. For the cases where $\underset{\sim}{x}$ is a current vector (Fig. 1(b) and 1(d)), these potential functions are the contents of N_a and N_b, respectively. Thus,

$$P_a(x_{a1},x_{a2},\ldots x_{aq}) = \int_0^{\underset{\sim}{x}_a} \underset{\sim}{y}_a(\underset{\sim}{x}_a)\cdot d\underset{\sim}{x}_a = \int_0^{\underset{\sim}{x}_a} \frac{\partial\phi(\underset{\sim}{x}_a)}{\partial \underset{\sim}{x}_a}\, d\underset{\sim}{x}_a = \phi(x_{a1},x_{a2}\ldots x_{aq}) \tag{7}$$

$$P_b(x_{b1},x_{b2}\ldots x_{bq}) = \int_0^{\underset{\sim}{x}_b} \underset{\sim}{y}_b(\underset{\sim}{x}_b)\cdot d\underset{\sim}{x}_b = \sum_{k=1}^{q}\left[\int_0^{x_{bk}} \left(\sum_{\ell=1}^{p} -g(-f_\ell)\frac{\partial f_\ell}{\partial x_{bk}}\right)dx_{bk}\right] =$$

$$= \sum_{\ell=1}^{p}\left[\int_0^{x_b} -g(-f_\ell)\sum_{k=1}^{q}\frac{\partial f_\ell}{\partial x_{bk}}\,dx_{bk}\right] = \sum_{\ell=1}^{p}\int_0^{-f_\ell} -g(-f_\ell)df_\ell = \sum_{\ell=1}^{p}\int_0^{w_{d\ell}} g(w_{d\ell})dw_{d\ell} \tag{8}$$

where $w_{d\ell} \triangleq v_{d\ell}$ in Fig. 1(a) and 1(c), and $w_{d\ell} \triangleq i_{d\ell}$ in Fig. 1(b) and 1(d).

The potential function associated with the composite q-port made up of the parallel connection of N_a and N_b is the sum of $P_a(\underset{\sim}{x}_a)$ and $P_b(\underset{\sim}{x}_b)$, where $\underset{\sim}{x}_a \triangleq \underset{\sim}{x}_b \triangleq \underset{\sim}{x}$, namely

$$P(x_1, x_2, \ldots x_q) = \phi(x_1, x_2, \ldots x_q) + \sum_{\ell=1}^{p} \int_0^{w_{d\ell}} g(w_{d\ell})\, dw_{d\ell} \qquad (9)$$

Now if we let $R_F \longrightarrow 0$ in Eq.(2) and let $G_B \longrightarrow 0$ in Eq.(3), the nonlinear resistors in N_b tend to the ideal diodes in the original circuit, and the integral in Eq.(9) is zero for $w_{d\ell} < 0$, and tends to zero as $w_{d\ell} \longrightarrow 0$ from the right. Hence,

$$\lim_{K \longrightarrow 0} P(x_1, x_2, \ldots x_q) = \phi(x_1, x_2, \ldots x_q) \qquad (10)$$

where $K \triangleq R_F$ or G_B.

It follows from Eq.(10) and the stationary theorems in [2] that the solution of every circuit in Fig. 1 is a stationary point of the scalar function $\phi(x_1, x_2 \ldots x_q)$. This important property can also be proved using the "penalty function" approach described in [3]. By assumption, $\phi(x_1, x_2, \ldots x_q)$ has only one stationary point and is a local minimum and hence the unique solution of the circuits in Fig. 1 is numerically equal to the global minimum of the objective function $\phi(x_1, x_2, \ldots, x_q)$, subject to the inequality constraints $f_j(x_1, x_2, \ldots, x_q) \geq 0$.

3. RELATIONSHIP WITH THE KUHN-TUCKER CONDITIONS

Kuhn-Tucker conditions have been shown to be necessary for solving constrained nonlinear programming problems [4]. It is interesting therefore to prove that the circuits proposed in Fig.1 simulate such conditions. To do this, note first that for each of the circuits in Fig.1, we have

$$
\begin{aligned}
w_{d\ell} &= -f_\ell(x_1, x_2, \ldots x_q) \leq 0 \quad , \quad \ell = 1,2,\ldots p \\
z_{d\ell} &\geq 0 \quad , \quad " \\
w_{d\ell} z_{d\ell} &= 0 \quad , \quad "
\end{aligned}
\tag{11}
$$

where $w_{d\ell}=v_{d\ell}$ and $z_{d\ell}=i_{d\ell}$ in Fig.1(a) and 1(b), and $w_{d\ell}=i_{d\ell}$ and $z_{d\ell}=v_{d\ell}$ in Fig.1(c) and 1(d), respectively.

Referring to the right-hand port, we can describe the k-port of all of the circuits in Fig.1 as,

$$
\frac{\partial \phi(x_1, x_2 \ldots x_q)}{\partial x_k} + \sum_{\ell=1}^{p} (-z_{d\ell}) \frac{\partial f_{d\ell}(x_1, x_2 \ldots x_q)}{\partial x_k} = 0 \tag{12}
$$

Identifying $-z_{d\ell}$ with a Lagrange multiplier, λ_ℓ^*, and assuming there is a unique solution, $\underset{\sim}{x}^*$, for the circuit, we can rewrite Eqs.(11)-(12) as follow:

$$
\begin{aligned}
&\frac{\partial \phi(\underset{\sim}{x}^*)}{\partial x_k} + \sum_{\ell=1}^{p} \lambda_\ell^* \frac{\partial f_\ell}{\partial x_k} = 0 \quad , \quad k=1,2,\ldots q \\
&f_\ell(\underset{\sim}{x}^*) \geq 0 \\
&\lambda_\ell^* \leq 0 \\
&\lambda_\ell^* f_\ell(\underset{\sim}{x}^*) = 0
\end{aligned}
\tag{13}
$$

Hence, the constraints imposed by the circuits in Fig. 1 are precisely the well-known Kuhn-Tucker conditions for solving a nonlinear programming problem, assuming that $\phi(.)$ and $f_\ell(.)$ are differentiable at $\underset{\sim}{x}^*$ and that the constraints on $f_\ell(.)$ satisfy some regularity conditions [4].

Although the Kuhn-Tucker conditions can be simulated by other circuits, those given in Fig. 1 are canonical in the sense that there is a one-to-one correspondence between the elements in Fig. 1 and the number of constraints in the Kuhn-Tucker conditions.

4. PRACTICAL CONSIDERATIONS

In this paper, the detailed physical implementation of the new circuits is not a major concern since essentially the same guidelines can be followed as given in [1]. Ideal diodes can be realized by a semiconductor diode embedded in the feedback loop of an op-amp, and the nonlinear controlled sources can be implemented by various combinations of op-amp's and multipliers [5]-[6].

The canonical circuits in Fig. 1 can be further simplified in the special case where each inequality constraint involves only a single variable of the form

$$x_k \geq 0 \quad , \quad k = 1,2,...q \tag{14}$$

In this case, the diode-controlled source combination on the left of Fig. 1(a)-(d) can be eliminated by connecting an ideal diode as shown in Fig. 2(a) for the canonical circuits in Fig. 1(a) and (c), or Fig. 2(b) for the canonical circuits in Fig. 1(b) and (d), respectively.

The implementation flexibility is one of the more interesting features that the new canonical circuits offer the designer. Cost and performance are highly influenced by the availability of circuit components for realizing each of the four alternative schemes. Note that two of the four circuits (namely, Fig. 1(b) and 1(c)) can be built using only one type of controlled sources. For example, we can first select the most convenient type of controlled sources, and then, realize an optimum op-amp implementation taking into account the differences in both cost and performance between a CCVS and a VCCS realization [5]-[6]. The optimum choice of a particular canonical circuit is illustrated below for the special but commom case of linear or quadratic programs.

In many applications, it is desirable to minimize an objective function

$$\phi(\underset{\sim}{x}) = \underset{\sim}{a}^T\underset{\sim}{x} + \frac{1}{2}\underset{\sim}{x}^T\underset{\sim}{B}\underset{\sim}{x} \tag{15}$$

subject to the affine inequality constraints

$$\underset{\sim}{f}(\underset{\sim}{x}) = \underset{\sim}{C}\underset{\sim}{x} - \underset{\sim}{d} > 0 \tag{16}$$

where $\underset{\sim}{a}$ and $\underset{\sim}{x}$ are q-vectors, $\underset{\sim}{f}(.)$ and $\underset{\sim}{d}$ are p-vectors, $\underset{\sim}{C}$ is a $(p \times q)$ matrix and $\underset{\sim}{B}$ is a $(q \times p)$ symmetric positive-definite matrix. When $\underset{\sim}{B}=\underset{\sim}{0}$, the resulting problem is called a linear program. Otherwise, we are dealing with a quadratic program.

Each circuit in Fig. 1(a)-(d) can be used to solve this problem. Figure 3 shows the four structures derived from Fig. 1(a)-(d) for simulating (15) and (16). Using $(\underset{\sim}{x}, \underset{\sim}{y})$ and $(\underset{\sim}{w}, \underset{\sim}{z})$ to denote the hybrid vectors associated with the right-hand ports and the left-hand ports of $\hat{N}$, respectively, we can describe $\hat{N}$ by:

$$\begin{bmatrix} \underset{\sim}{z} \\ \underset{\sim}{y} \end{bmatrix} = \begin{bmatrix} \underset{\sim}{0} & \underset{\sim}{C} \\ -\underset{\sim}{C}^T & \underset{\sim}{0} \end{bmatrix} \begin{bmatrix} \underset{\sim}{w} \\ \underset{\sim}{x} \end{bmatrix} \tag{17}$$

Note that for the circuits in Fig. 3(a) and 3(d), $\hat{N}$ is a (p+q)-port transformer. However, $\hat{N}$ is a <u>current-controlled</u> (resp., <u>voltage-controlled</u>) (p+q)-port in Fig. 3(b) (resp. 3(c)). Also, note that $\hat{R}$ is a linear circuit, which is the same for all cases in Fig. 3. Diodes and dc independent sources are used to load the left-hand ports of $\hat{N}$ and to connect its right-hand ports with $\hat{R}$.

Comparing these 4 alternative realizations, it is logical to choose either Fig. 3(b) or 3(c) since the (p+q)-port requires a hybrid realization, which is much more complicated. The final choice will

depend on the cost of implementing a current-controlled or a voltage-controlled n-port using the existing technology.

5. CONCLUSIONS

We have shown that the circuit reported in [1] is not the only canonical circuit capable of solving any nonlinear programming problem. Thus, a family of circuits has been presented here, explicitly specifying its four canonical elements. In fact, since they only use one kind of controlled sources, the circuits in Fig. 1(b) and 1(c) are only x-controlled canonical circuits.

The validity of the three new canonical circuit structures (Fig. 1(b),(c),(d)) has been verified by simulating several nonlinear programming problems using the general-purpose computer program SPICE2. The simulation results are consistent with those reported in [1] and [3].

6. REFERENCES

[1] L.O. CHUA and G.N. LIN, "Nonlinear Programming without computation". IEEE Trans. on CAS, vol.Cas-31, n 2, pp.182-188, Feb. 1984.

[2] L.O. CHUA, "Stationary principles and potential functions for nonlinear networks", J. Franklin Inst., vol 296, n 2, pp.91-114, Aug. 1973.

[3] L.O. CHUA and G.N. LIN, "Nonlinear optimization with constraints: a cookbook approach". Int. J. Circuit Theory Appl., vol.11, pp.141-159, 1983.

[4] O.L. MANGASARIAN, "Nonlinear Programming". New York: McGraw-Hill, 1969.

[5] J.L. HUERTAS, J.I. ACHA and A. GAGO, "Design of general voltage or current controlled resistive elements and their applications to the synthesis of nonlinear networks", IEEE Trans. on CAS, vol.CAS-27, n 2, pp.92-103, Feb. 1980.

[6] J.L. HUERTAS and A. GAGO, "On the realization of arbitrary linear resistive n-port network", IEE J. Electronic Circuits and Syst., vol.3, n 6, pp.247-252, Nov. 1979.

FIGURE CAPTIONS.

Figure 1: Canonical nonlinear programming circuits.

Figure 2: Circuits for imposing constraint (14).

Figure 3: Canonical quadratic programming circuits.

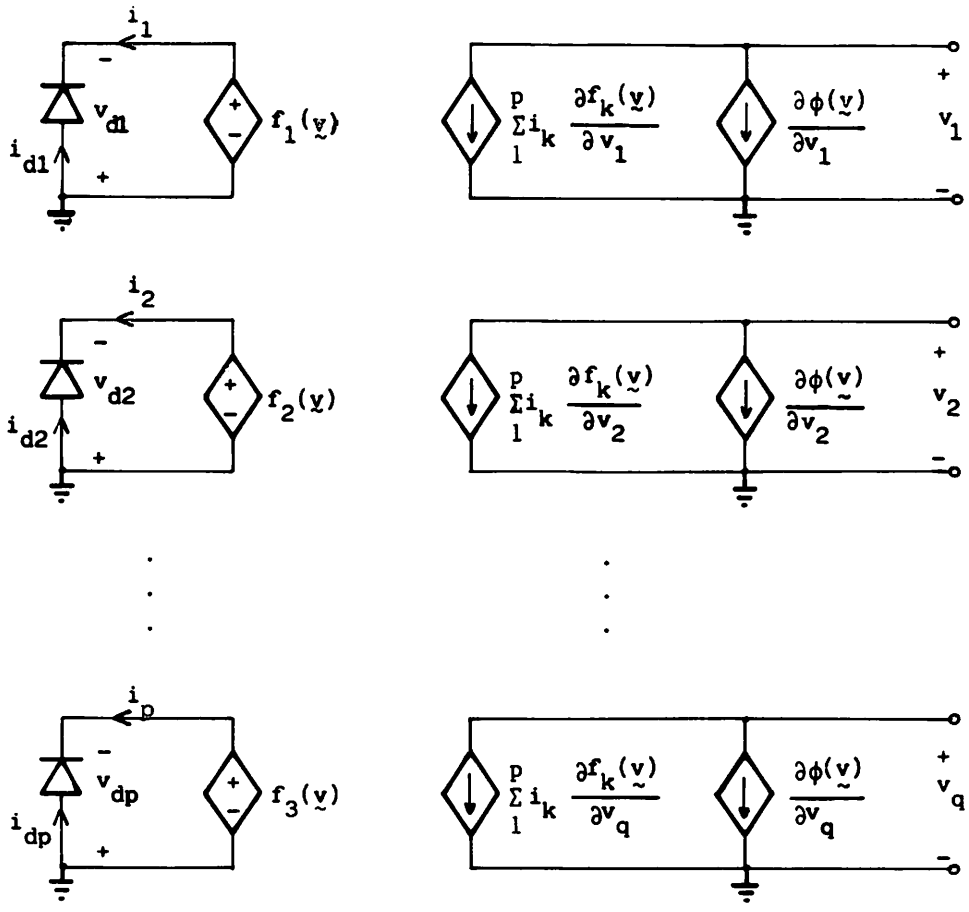
i_1
v_{d1}
i_{d1}
$f_1(\underset{\sim}{v})$
$\sum_1^p i_k \frac{\partial f_k(\underset{\sim}{v})}{\partial v_1}$
$\frac{\partial \phi(\underset{\sim}{v})}{\partial v_1}$
v_1
i_2
v_{d2}
i_{d2}
$f_2(\underset{\sim}{v})$
$\sum_1^p i_k \frac{\partial f_k(\underset{\sim}{v})}{\partial v_2}$
$\frac{\partial \phi(\underset{\sim}{v})}{\partial v_2}$
v_2
i_p
v_{dp}
i_{dp}
$f_3(\underset{\sim}{v})$
$\sum_1^p i_k \frac{\partial f_k(\underset{\sim}{v})}{\partial v_q}$
$\frac{\partial \phi(\underset{\sim}{v})}{\partial v_q}$
v_q

(a)

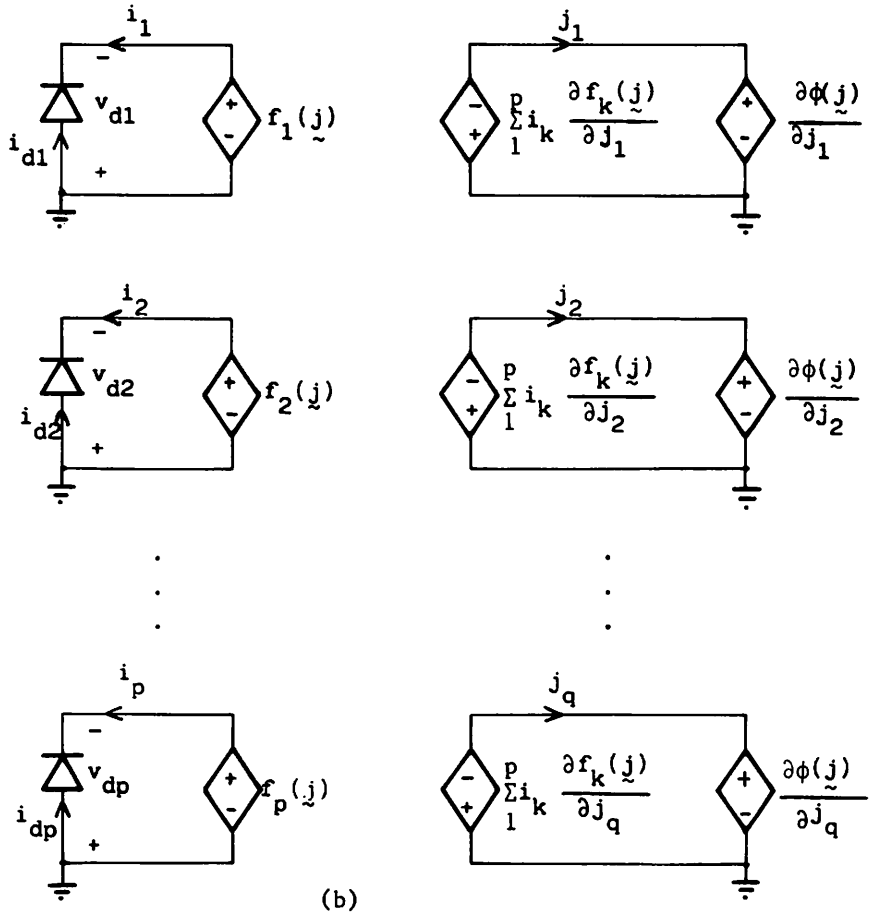
i_1
v_{d1}
i_{d1}
$f_1(\underset{\sim}{j})$
j_1
$\sum_1^p i_k \frac{\partial f_k(\underset{\sim}{j})}{\partial j_1}$
$\frac{\partial \phi(\underset{\sim}{j})}{\partial j_1}$
i_2
v_{d2}
i_{d2}
$f_2(\underset{\sim}{j})$
j_2
$\sum_1^p i_k \frac{\partial f_k(\underset{\sim}{j})}{\partial j_2}$
$\frac{\partial \phi(\underset{\sim}{j})}{\partial j_2}$
i_p
v_{dp}
i_{dp}
$f_p(\underset{\sim}{j})$
j_q
$\sum_1^p i_k \frac{\partial f_k(\underset{\sim}{j})}{\partial j_q}$
$\frac{\partial \phi(\underset{\sim}{j})}{\partial j_q}$

(b)

Fig. 1

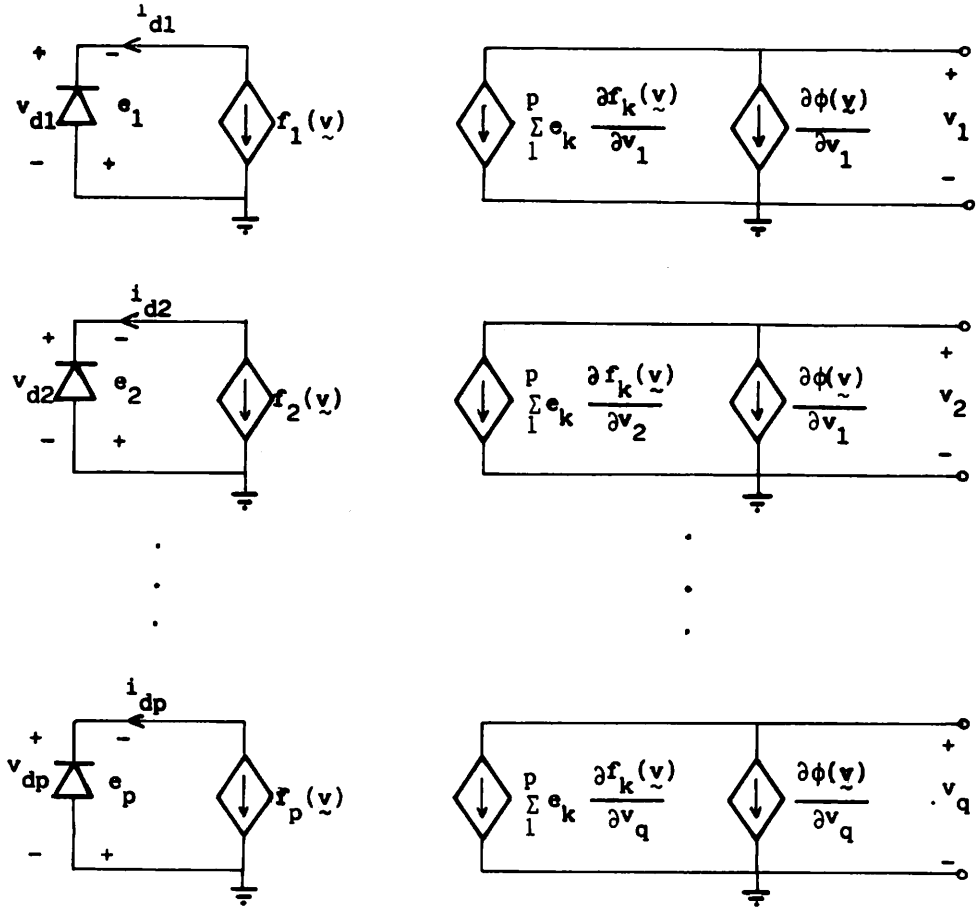
i_{d1}
v_{d1}
e_1
$f_1(\underset{\sim}{v})$
$\sum_1^p e_k \frac{\partial f_k(\underset{\sim}{v})}{\partial v_1}$
$\frac{\partial \phi(\underset{\sim}{v})}{\partial v_1}$
v_1
i_{d2}
v_{d2}
e_2
$f_2(\underset{\sim}{v})$
$\sum_1^p e_k \frac{\partial f_k(\underset{\sim}{v})}{\partial v_2}$
$\frac{\partial \phi(\underset{\sim}{v})}{\partial v_1}$
v_2
i_{dp}
v_{dp}
e_p
$f_p(\underset{\sim}{v})$
$\sum_1^p e_k \frac{\partial f_k(\underset{\sim}{v})}{\partial v_q}$
$\frac{\partial \phi(\underset{\sim}{v})}{\partial v_q}$
v_q

(c)

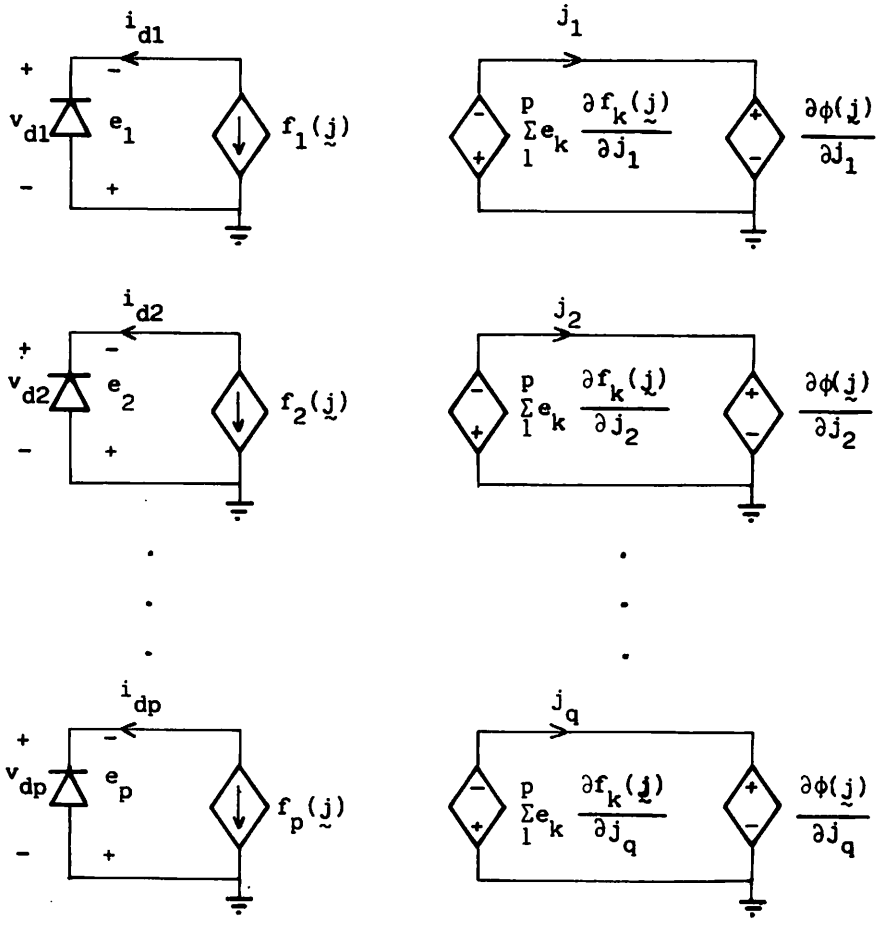
i_{d1}
v_{d1}
e_1
$f_1(\underset{\sim}{j})$
j_1
$\sum_1^p e_k \frac{\partial f_k(\underset{\sim}{j})}{\partial j_1}$
$\frac{\partial \phi(\underset{\sim}{j})}{\partial j_1}$
i_{d2}
v_{d2}
e_2
$f_2(\underset{\sim}{j})$
j_2
$\sum_1^p e_k \frac{\partial f_k(\underset{\sim}{j})}{\partial j_2}$
$\frac{\partial \phi(\underset{\sim}{j})}{\partial j_2}$
i_{dp}
v_{dp}
e_p
$f_p(\underset{\sim}{j})$
j_q
$\sum_1^p e_k \frac{\partial f_k(\underset{\sim}{j})}{\partial j_q}$
$\frac{\partial \phi(\underset{\sim}{j})}{\partial j_q}$

(d)

Fig. 1

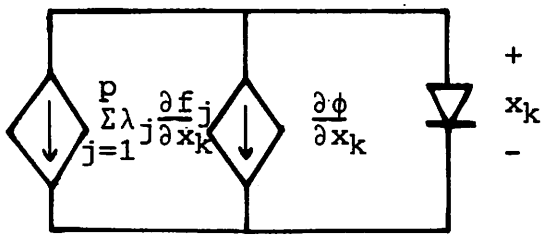
$\sum_{j=1}^{p} \lambda_j \frac{\partial f_j}{\partial x_k}$
$\frac{\partial \phi}{\partial x_k}$
+
x_k
-

(a)

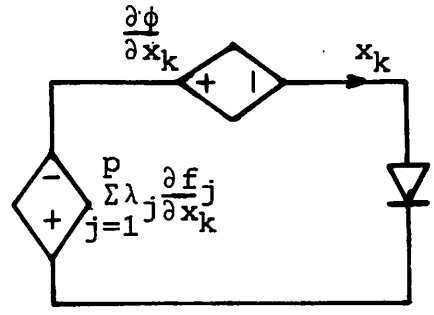
$\frac{\partial \phi}{\partial x_k}$
+ 1
x_k
-
+
$\sum_{j=1}^{p} \lambda_j \frac{\partial f_j}{\partial x_k}$

(b)

Fig. 2

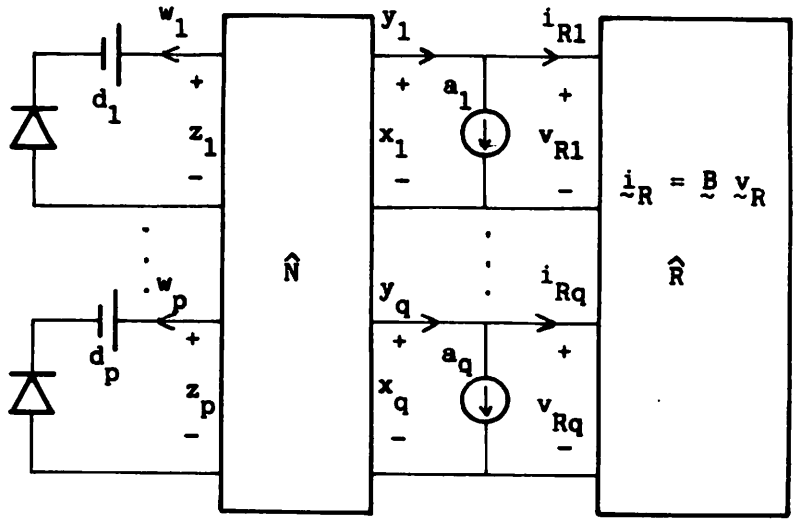
w_1
d_1
z_1
w_p
d_p
z_p
$\hat{N}$
y_1
x_1
a_1
i_{R1}
v_{R1}
y_q
x_q
a_q
i_{Rq}
v_{Rq}
$\underset{\sim}{i}_R = \underset{\sim}{B}\ \underset{\sim}{v}_R$
$\hat{R}$

(a)

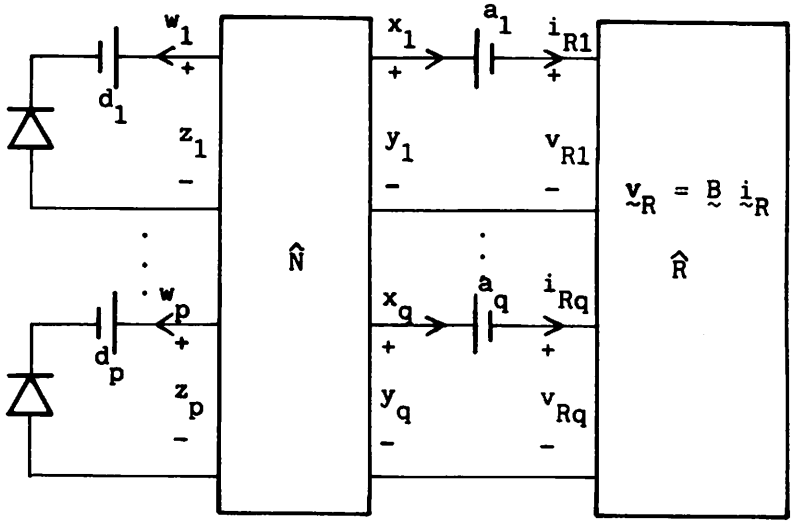
w_1
d_1
z_1
w_p
d_p
z_p
$\hat{N}$
x_1
a_1
i_{R1}
y_1
v_{R1}
x_q
a_q
i_{Rq}
y_q
v_{Rq}
$\underset{\sim}{v}_R = \underset{\sim}{B}\ \underset{\sim}{i}_R$
$\hat{R}$

(b)

Fig. 3

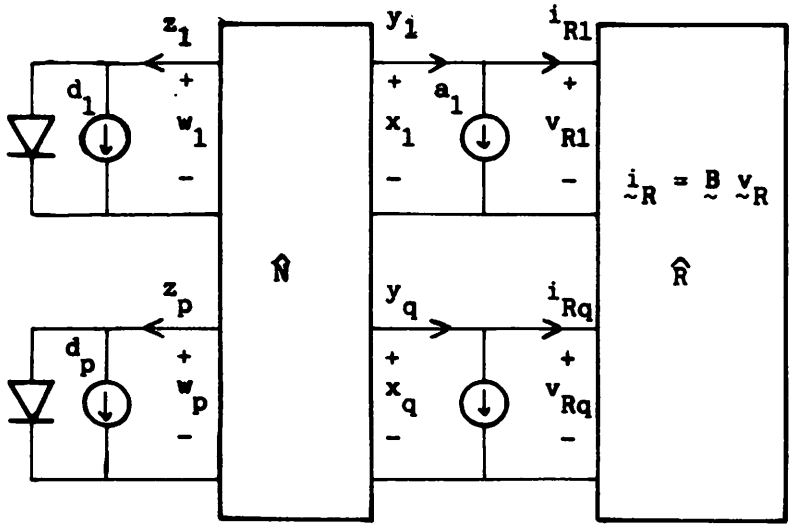
z_1
y_1
i_{R1}
d_1
w_1
x_1
a_1
v_{R1}
$\underset{\sim}{i}_R = \underset{\sim}{B}\ \underset{\sim}{v}_R$
$\hat{N}$
$\hat{R}$
z_p
y_q
i_{Rq}
d_p
w_p
x_q
v_{Rq}

(c)

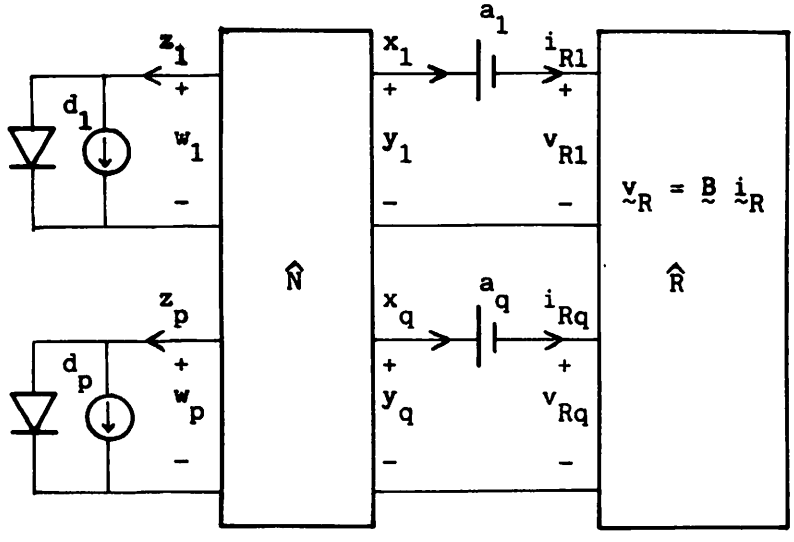
a_1
z_1
x_1
i_{R1}
d_1
w_1
y_1
v_{R1}
$\underset{\sim}{v}_R = \underset{\sim}{B}\ \underset{\sim}{i}_R$
$\hat{N}$
$\hat{R}$
z_p
x_q
a_q
i_{Rq}
d_p
w_p
y_q
v_{Rq}

(d)

Fig. 3